European Journal of Pharmaceutics and Biopharmaceutics 134 (2019) 77–87

Contents lists available at ScienceDirect

European Journal of Pharmaceutics and Biopharmaceutics

journal homepage: www.elsevier.com/locate/ejpb

Research paper

Conversion of PLGA nanoparticle suspensions into solid dosage forms via fluid bed granulation and tableting

Lutz Horster[a], Alexander Bernhardt[b], Kevin Kiehm[a], Klaus Langer[b,*]

[a] Rottendorf Pharma GmbH, Ostenfelder Straße 51-61, 59320 Ennigerloh, Germany
[b] Institute of Pharmaceutical Technology and Biopharmacy, University of Muenster, Corrensstraße 48, 48149 Münster, Germany

ARTICLE INFO

Keywords:
Polymeric nanoparticles
Drug delivery system
Fluid bed granulation
Design of experiment
Tableting
In vitro release

ABSTRACT

Incorporating poorly soluble drugs into polymeric nanoparticles is a widely investigated approach to improve their biopharmaceutical performance. Poly(DL-lactide-*co*-glycolide) (PLGA) nanoparticle formulations have previously been tested and recommended as drug carriers for peroral administration of poorly soluble porphyrin derivatives intended for photodynamical therapy. Based on those PLGA formulations the present study investigates conventional techniques like fluid bed granulation and tableting for conversion of such polymeric nanoparticle suspensions into solid dosage forms. Analytical methods like asymmetrical flow field-flow fractionation (AF4) and photon correlation spectroscopy (PCS) were used to assess changes of the nanoparticle properties during processing and the recovery after redispersion of the solid dosage forms. Preliminary experiments were conducted to demonstrate the feasibility of the granulation and tableting strategy. Afterwards, design of experiments (DoE) was used to determine formulation and process parameters with critical influence on several properties of the solid forms, in particular the recovery of nanoparticles during dissolution testing.

Fluid bed granulation with aqueous PLGA nanoparticle suspensions and soluble carriers was shown to be a simple and high yield process for drying of the nanoparticles. The nanoparticle concentration of the granulation suspension and the ratio of the spraying rate and the atomization air pressure were critical for the physicochemical characteristics of the granules like density and particle size distribution (PSD) as well as for the redispersibility to nanoparticle suspensions of original properties. The granules were compressed to tablets without impairing the nanoparticle diameter and the recovery when an adequate level of filler and low compression forces were used.

1. Introduction

Nanoparticulate drug carriers are intensively investigated as carriers for lipophilic drug substances, especially for tumor therapy due to enhanced permeability and retention effect (EPR) [1–3]. Such polymeric nanoparticles for drug delivery most commonly consist of biodegradable materials such as poly(lactic-*co*-glycolic acid) (PLGA) [4,5].

Peroral administration of drugs is the preferred route for dosage forms due to advantages in the manufacturing as well as the improved patient compliance. While most work with polymeric nanoparticles has been focused on intravenous administration, several studies have investigated polymeric nanoparticles for peroral administration of drugs like curcumine [6], cyclosporine [7], exendin-4 [8], insulin [9–11], nifedipine [12] or paclitaxel [13]. Several approaches for the modification of polymeric nanoparticles have been followed to overcome the challenges linked to the gastrointestinal barrier, including the combination with mucolytic agents [14], densely charged surfaces [15] and PEG coatings [16]. It seems not absolutely clear whether improvements in bioavailability observed after use of those nanoparticulate drug delivery systems require intact nanoparticles to cross the intestinal mucus layer and be absorbed [9,17,18] or if they can occur just due to prolonged drug release at the mucosal barrier [19]. However, polymeric nanoparticles for peroral administration and suitable dosage forms thereof are a field of high interest.

As nanoparticle suspensions are disadvantageous in means of stability, they are often dried to avoid aggregation and sedimentation during storage. Most common drying techniques are freeze- and spray-drying or combinations thereof [4,20,21]. The dried intermediates obtained by those techniques often show powder characteristics which are unfavorable for further downstreaming. Wet granulation with

* Corresponding author.
E-mail addresses: lutz.horster@rottendorf.com (L. Horster), a.bernhardt@uni-muenster.de (A. Bernhardt), kevin.kiehm@rottendorf.com (K. Kiehm), k.langer@uni-muenster.de (K. Langer).

https://doi.org/10.1016/j.ejpb.2018.11.011
Received 13 July 2018; Received in revised form 7 October 2018; Accepted 13 November 2018
Available online 14 November 2018
0939-6411/

nanoparticle suspensions or intermediates that contain nanoparticles can lead to nanocomposite microparticles of better flowability. Fluid bed granulation is one possibility of drying nanosuspensions. Several authors investigated fluid bed processing for transforming nanoscale drug delivery systems like nanocrystal suspensions or self-micro-emulsifying drug delivery systems (SMEDDS) into solid form [22–26]. Though, drying of polymeric nanoparticles via fluid bed processing is rarely mentioned. Only few studies deal with the processing of dried intermediates containing polymeric nanoparticles into solid dosage forms with the aim of obtaining the original nanoparticles after redispersion [27–29]. Systematic evaluation of the parameters by DoE is common in the area of pharmaceutical fluid bed processing [30–33] and also increasingly used related to polymeric nanoparticles [34–36]. Still, in connection with fluid bed drying of polymeric nanoparticles and further downstreaming, DoE is not described so far to the best of our knowledge.

The present study focuses on peroral dosage forms delivering PLGA nanoparticles with the same characteristics as present in the original suspensions and manufactured using conventional down-streaming strategies like fluid bed processing with subsequent tableting or encapsulation.

2. Materials and methods

2.1. Materials

PLGA characterized by a copolymer ratio of 50:50 (Resomer® RG 502H) was purchased from Evonik Industries (Darmstadt, Germany). Other materials purchased were α-lactose-monohydrate (GranuLac® 70 (Lac) from Molkerei Meggle, Germany and Pharmatose® 200 (Lac_{200}) from DMV, Germany), dibasic calcium phosphate (DCPA) (A-Tab® from Innophos Inc., USA), polyethylene glycol 6000 (PEG) (Lipoxol® 6000 Med Powder from Sasol, Germany), microcrystalline cellulose (MCC) (Avicel® PH 102) and croscarmellose sodium (CMC) (Ac-Di-Sol® SD711 from FMC BioPolymer, Ireland), sodium stearyl fumarate (SSF) (Pruv® from JRS Pharma, Germany), poly(vinyl alcohol) (PVA4-88, molecular weight 31 kDa, or 8-88, molecular weight 67 kDa, from Merck, Germany). Poloxamer (P188) (Kolliphor® P188 from BASF, Germany), silica (SiO_2) (Syloid® 244 FP from Grace, USA) and size 0 HPMC capsules (VCaps® plus from Capsugel, Belgium) were obtained as gift. Purified water (PW) was used as obtained either from pharma water installation or PureLab flex (ELGA, UK). All solvents and other reagents were of analytical grade and used as obtained.

2.2. Preparation and characterization of PLGA nanoparticles

2.2.1. Preparation of PLGA nanoparticles

Nanoparticles based on PLGA were formed by a well-established emulsion diffusion method as previously described [37]. Briefly, PLGA solutions in ethyl acetate (10% (w/v)) were emulsified with double the amount of aqueous PVA solution (1% (w/v)) using an Ultra-Turrax® T25 digital (tooling S25-19G, IKA, Germany) at 24,000 rpm for 20 min. The resulting primary dispersions were diluted with PVA solution to achieve the desired theoretic nanoparticle concentration and stirred on a magnetic stirrer to evaporate the organic solvent for 14–23 h.

2.2.2. Physicochemical characterization of PLGA nanoparticles

2.2.2.1. Gravimetric determination of the nanoparticle content. The nanoparticle content was determined gravimetrically by transferring aliquots of 50.0 µL of the nanoparticle suspensions and PVA solutions into trays and drying them to constant mass at 80 °C.

2.2.2.2. Photon correlation spectroscopy (PCS). The average particle diameter and the polydispersity index (PDI) were determined by PCS using a Malvern Zetasizer Nano ZS system (Malvern Instruments Ltd., Malvern, UK). Diluted samples were measured at a temperature of 22 °C, a backscattering angle of 173°, a measurement position of 4.65 mm and an attenuator value of 6.

2.2.2.3. Scanning electron microscopy (SEM). For SEM, the particle suspensions and the suspensions prepared from the solid dosage forms were diluted with purified water to obtain a particle concentration of around 0.25 mg/ml. The dispersions were dropped on a filter (MF-Millipore™ membrane filter VSWP, 0.1 µm) and dried for 24 h in a desiccator. Afterwards the membranes were sputtered with gold under argon atmosphere (SCD 040, BAL-TEC, Balzers, Liechtenstein) to gain electric conductivity. The SEM pictures were received with an accelerating voltage of 10 kV and a working distance of 10 mm.

2.3. Preparation and characterization of nanoparticle containing solid forms

2.3.1. Preparation of PLGA nanoparticle containing granules

The granules were produced using MIDI Glatt fluid bed granulators in top spray mode (Glatt, Germany). Different carriers in quantities to achieve lots of 0.17 kg granules were loaded into the pre-warmed product bowl. Mostly one single excipient was used as the carrier. However, in few cases also mixtures were used as carrier that in addition to Lac either contained 5% P188 or 3% SiO_2 (percentage amount of these additives in relation to the batch size of 0.17 kg). The spraying of the nanoparticle suspension was started directly after starting the fluidization process. The air flow rate was chosen to obtain a fluidized bed. The inlet air temperature was adapted to keep the product temperature at around 25 °C. This was done to hold the process temperature below the glass transition temperature of the used PLGA nanoparticles, though earlier trials had shown that slightly exceeding this temperature range up to 37 °C product temperature did not negatively influence the product properties. After spraying the desired quantity of the nanoparticle suspension, the granules were dried, unloaded and weighed.

2.3.2. Physicochemical characterization of nanoparticle containing granules

The granules were characterized with respect to their moisture (MA45, Sartorius, Germany), bulk and tapped density (Erweka, Germany), flowability (based on angle of repose), and particle size distribution (Analysette 3 Pro, Fritsch GmbH, Germany). Approximate mean particle size in microns was determined from percentage residue and mean sieve class in microns as follows:

$$\text{approximate mean particle size } [\mu m] = \frac{\Sigma(\text{mean sieve class} \times \text{residue})}{100}$$

2.3.3. Tableting and encapsulation of nanoparticle containing granules

For preparation of the final blends, the excipients were sieved over a 500 µm screen and mixed with the granules using a LM20 free fall blender (L.B. Bohle GmbH, Germany) at 19 to 21 rpm for 13 min. The blends consisted of 50–95% granules, 0–45% MCC, 2.9% PEG as soluble lubricant in addition with 0.1% SSF, and 2% of CMC as disintegrant. Classical metal lubricants, e.g. magnesium stearate and high amounts of fine insoluble excipients were avoided to prevent issues during qualitative and quantitative analysis of the released nanoparticles. Final blends were manually compressed to tablets of 500 mg weight using a rotary tablet press (Kilian Eifel, Kilian GmbH, Germany) with a 11.5 r 12.5 mm tooling. HPMC capsules were filled with granules or final blend and closed using a manual capsule filling machine. In case the final blends were encapsulated, plugs were manually preformed via a tamping machine with a size 0 punch at 60 N.

2.3.4. Physicochemical characterization of nanoparticle containing tablets

The tablets were characterized with respect to their dimensions (digital caliper, Mitutoyo Deutschland GmbH, Germany), weight

(PB153-S/FACT, Mettler Toledo GmbH, Germany), disintegration time (ZT 304, Erweka GmbH, Germany), breaking strength (PTB 302, Pharma Test Apparatebau AG, Germany), moisture content (MA45, Sartorius AG, Germany; 5 g, 85 °C, automatic end at < 5 mg/24 s), and friability (F1 USP, Sotax AG, CH).

2.3.5. Dissolution test of nanoparticle containing dosage forms

In vitro dissolution tests of the nanoparticle-containing granules and tablets were performed using an USP apparatus II (DT600, Erweka GmbH, Germany). Samples corresponding to 10–40 mg NP were placed in 500 ml purified water (PW) of 37 ± 1 °C at a paddle stirring rate of 50 rpm. At predetermined time points from 2 to 120 min, 2 ml aliquots of dissolution medium were withdrawn and replaced with PW.

2.3.6. Asymmetric flow-field-flow fractionation (AF4)

An established method [29] was used to determine nanoparticle recovery via AF4. The system consisted of an AF 2000 module box, channel oven (PN4020), autosampler (PN5300), solvent organizer and degasser (PN7140 and PN7520), two high performance liquid chromatography pumps (PN1130), and a multi angle light scattering (MALS) detector (PN3070). All components were purchased from Postnova Analytics (Landsberg am Lech, Germany). The channel consisted of an acrylic glass plate, a polyetheretherketone (PEEK) spacer with 350 µm thickness and 27.7 cm length and a channel block with a ceramic frit. The channel was used with a regenerated cellulose membrane with a 10 kDa cut-off. The temperature of the channel oven was set to 25 °C. SIF_{SP} (pH 6.8) was used as the mobile phase. Slight deviations were made to the method. The cross-flow profile is presented in Table 1. During the focusing step, the injection flow was set to 0.2 ml/min. The detector flow rate was constant at 0.5 ml/min. MALS signals were evaluated at 90°. Quantitative analysis was performed by Clarity Software (Version 2.6, DataApex, Prague, Czech Republic).

2.3.7. Photon correlation spectroscopy (PCS)

The samples were analyzed for quantification without further treatment using a PCS method with fixed experimental settings (attenuator 8, position 4.65 mm, 15 runs of 10 s, at a backscattering angle of 173°). The method was validated for several batches of nanoparticles (data not shown).

If not mentioned otherwise, the results for the particle size and nanoparticle recovery below were obtained by the PCS method.

2.4. Design of experiments (DoE)

The granulation and tableting procedure described above were performed to obtain information about the influence of the selected process parameters on the physicochemical and reconstitution properties. A three-factor two-level design (2^3) with three central point experiments was used with the factors spraying rate (A), atomization air pressure (B), and nanoparticle content of final granules (C). Parameters kept as constant as possible were the type of stabilizing PVA (type 4-88), the carrier type (Lac), the product temperature (25 °C), and the amount of suspension to be sprayed. The latter was adjusted in a narrow range of 410–445 ml based on the gravimetrically determined nanoparticle content of the suspension to attain the desired nanoparticle load. The factor levels were set on the basis of preliminary experiments. Minitab® software (version 17, Minitab Inc., USA) was used to generate and evaluate the design that was performed in a randomized order. Significant ($p < 0.05$) terms according to analysis of variance were chosen for final evaluation.

A two-factor two-level design with central point and multiple regression were used for tableting of all respective sub lots of the DoE granules. The influence of the breaking strength and the amount of plastic filler on the response variable recovery of nanoparticles during dissolution was evaluated.

Table 1
Cross flow profile to determine NP recovery via AF4.

Time [min]	Step	Cross flow [ml/min]	Profile
0	Focusing	1.0	constant
5.0	Transition	1.0	constant
5.2	Elution	1.0	constant
6.7		1.0	power function: 0.2
21.7		0.1	constant
66.7	Rinse	0.0	constant
84.7	Rinse	0.1	linear
85.7	Rinse	0.1	constant
95.7	End		

3. Results and discussion

3.1. Preliminary tests for setting of formulation and process parameters

The present study evaluated the downstreaming of aqueous PLGA nanoparticle suspensions to oral solid dosage forms with conventional methods. It also evaluated the influence of different formulation and process parameters on the incorporated particles. An established standard formulation of unloaded PLGA nanoparticle suspensions was used throughout the experiments to reduce the variance of nanoparticle quality due to a batch to batch variability of the nanoparticle suspension. The formulation was only altered with respect to the content of PLGA (2.5 or 5.0%) and the molecular mass of stabilizing agent PVA (4-88 or 8-88).

The first step of the downstreaming process was a fluid bed granulation approach that was performed in top spray mode for all batches. This was intended to avoid any formation of smooth films which are reported for bottom spray processing [25,38]. The described effect is a coalescence of PLGA nanoparticles into larger films which are generated during processing. This effect is assumed to be irreversible and any deagglomeration is unlikely to occur. The stabilizer (PVA) was intended to work as a binder during granulation. Its use for parenteral application may be inadequate especially due to lack of degradation. However, for peroral use, no such restriction exists, and the polymer is widely used as a sustained release agent, in coating formulations and in hot melt processes [39,40].

3.1.1. Choice of method for quantification of released nanoparticles

AF4, PCS and SEM were used to evaluate the release of unloaded PLGA nanoparticles from the granules. The AF4 technique has been widely used for characterization of nanoparticles and has already been validated for quantification of unloaded PLGA nanoparticles [29]. This method was shown to work for the dosage forms prepared in the present study, when calibrated with an aliquot of the original nanoparticle suspension batch. Still, the *per se* non-quantitative PCS technique was tested as a time saving alternative quantification method due to the large number of samples. SEM was only used to complement the quantitative tools as it gave only rough information about changes of the nanoparticle size and the occurrence of agglomerates.

A suitable correlation between the PCS count rate and the nanoparticle concentration was achieved for 14 PLGA nanoparticle preparations with little batch to batch variability in particle diameter (198 ± 5 nm) and PDI (0.068 ± 0.013) (Fig. 1). The PCS method was therefore calibrated for the used concentration range. As shown in Fig. 2, the PCS led to similar results compared to the AF4 when used for the quantification of the same samples. Both methods were validated for the investigated nanoparticles. However, the use of this technique might be limited to formulations as simple as the tested ones. The formulations used for this study had quite a high load of nanoparticles. They also did not include excipients or carriers of high viscosity or light scattering properties that might falsify the measurement (e.g. gelatin

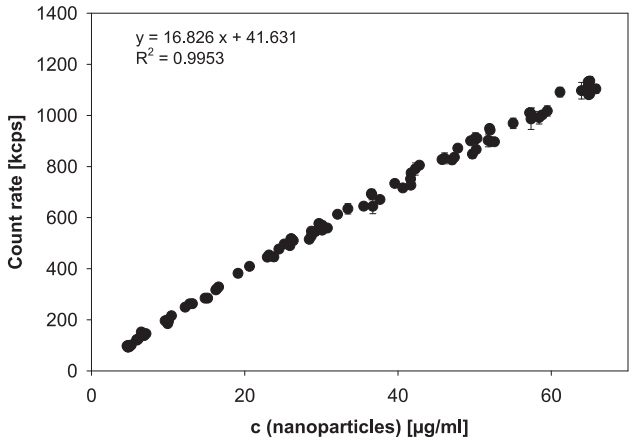

Fig. 1. Calibration of PCS method with 14 nanoparticle suspensions (each ≥ 4, mean values ± SD).

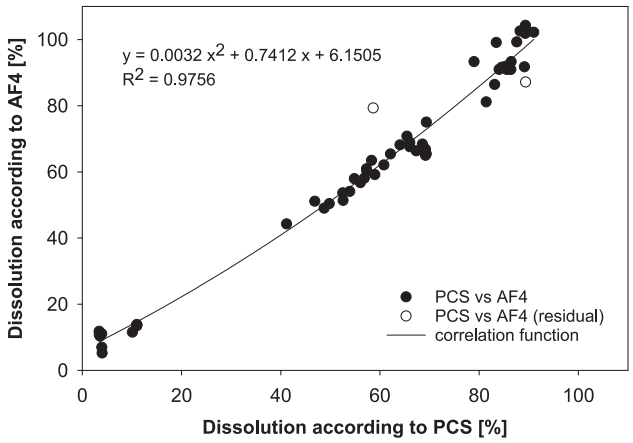

Fig. 2. Comparison between recovery results of nanoparticle containing granules and tablets obtained by PCS and AF4.

capsules, higher amounts of nanoparticulate inorganic materials like SiO_2). If nothing else is stated, the following results were measured by PCS for the recovery of the nanoparticles and the results represent the mean percentage recovery of nanoparticles after 120 min of dissolution testing.

3.1.2. Choice of excipients and process parameters for granulation

For the first feasibility tests, carriers of different lactose grades and DCPA were used. SEM revealed that only the pure soluble carriers led to relevant recovery of single nanoparticles similar to the original suspension (Fig. 3A). On the surface of lactose-based granules individual nanoparticles were detected (Fig. 3B/C) and were isolated from dissolution media (Fig. 3D). On the other hand, on the surface of DCPA, PLGA nanoparticles rather seemed to coalesce than to stick to the granuleś surface (Fig. 3E). The addition of poloxamer to the lactose improved the flowability of the granules but likewise led to particle coalescence (Fig. 3F) and a decreased nanoparticle recovery (Table 2). This was attributed to the formation of a lubricating film and a change of the surface hydrophobicity that is generally critical in coating processes [23,41]. Therefore, a simple formulation with lactose as a single carrier seemed most suitable so far.

The nanoparticle recovery from such lactose granules was only around 70% at its best. Hence, a relevant part of the nanoparticles (~30%) was not detectable and most likely had agglomerated during the drying step. The nanoparticle level of the suspension posed another adjustable formulation parameter that was varied to further improvement of the nanoparticle recovery. The content of the nanoparticles in the granules was kept the same. However, a larger volume of diluted suspension was used for spraying leading to a higher content of the stabilizer. Even larger and looser granules were expected when spraying larger volumes of suspension. The less viscous PVA type PVA 4-88 was therefore tested as alternative stabilizer to prevent the generation of unreasonably coarse granules. Actually, the use of a larger volume of less concentrated suspension led to increased recovery values (Table 2, batch 6). Later trials confirmed that this positive effect was dependent on the decreased nanoparticle concentration of the suspension and not on the use of the new stabilizer type: a granulation trial with diluted suspension with PVA 8-88 (batch 7) led to an optimized recovery. In contrast, a process with the new stabilizer PVA 4-88 but in a concentrated nanoparticle suspension analogue to batch 3 (batch 8) resulted in no further improvement. Granules produced with PVA 8-88 showed a slightly higher nanoparticle recovery with the same process conditions compared to granules produced with PVA 4-88. However, the granules with PVA 4-88 showed more desirable powder

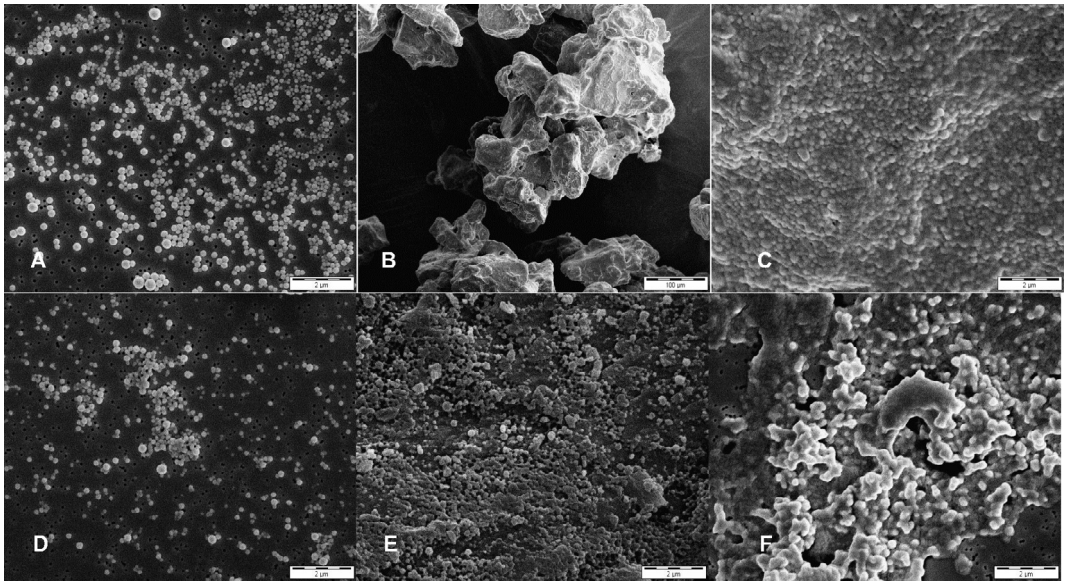

Fig. 3. SEM pictures of PLGA NP suspension (A), surface of Lac granules (B, C), dissolution medium after 50 min dissolution of a tablet containing Lac granules (D), surface of DCPA granules (E), redispersed Lac/P188 granules (F).

Table 2
Settings and results of preliminary granulation experiments.

Batch [no]	Carrier	PVA type	PVA content of granules [%]	Product temperature [°C]	PLGA content of granules [%]	Spraying rate [g/min]	Atomization air pressure [bar]	Yield [%]	Mean particle size [µm]	Bulk density [g/ml]	Flowability [cot°]	NP release [%]
1	Lac	8–88	1.1	35	4.7	3.4	0.8	99	379	0.27	1.14	69 ± 1
2	Lac/P188	8–88	1.1	35	5.1	3.4	0.8	99	369	0.27	1.19	11 ± 0
3	Lac	8–88	1.1	25	5.3	3.2	0.8	97	445	0.25	1.16	69 ± 5
4	Lac/P188	8–88	1.1	25	5.3	4.2	0.8	99	412	0.30	1.28	4 ± 0
5	DCPA	8–88	1.0	25	5.1	4.0	0.8	98	249	0.39	1.22	4 ± 0
6	Lac	4–88	2.5	25	5.8	3.2	0.8	97	525	0.23	1.14	86 ± 1
7	Lac	8–88	2.2	25	5.5	3.2	0.8	97	533	0.20	1.00	95 ± 1
8	Lac	4–88	1.2	25	5.2	3.1	0.8	98	379	0.26	1.14	49 ± 1
9	Lac/SiO_2	4–88	2.4	25	5.5	3.1	0.8	91	382	0.25	1.19	62 ± 2
10	Lac_{200}	4–88	2.4	25	5.4	3.2	0.8	97	323	0.19	1.14	95 ± 1

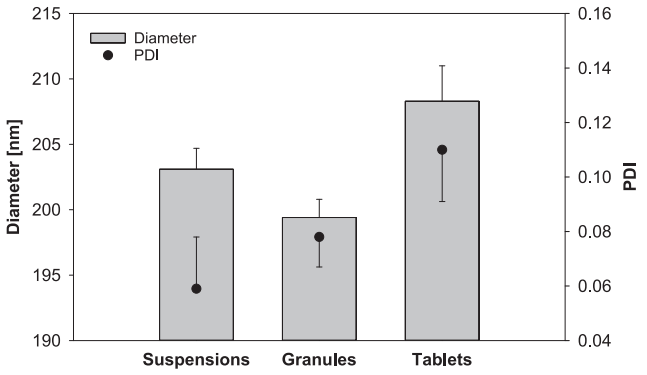

Fig. 4. Mean diameter (bars) and PDI (circles) values of nanoparticles after preparation and reconstitution from granules and tablets (mean ± SD, n ≥ 3 for 19 lots). For the sake of clarity the standard deviation bars were depicted in one direction.

characteristics of a smaller mean particle size and a higher density. These differences between the granules were mainly attributed to the different viscosity of the two types of the steric stabilizer. In the end, PVA 4-88 was chosen as stabilizer for further experiments.

The inclusion of colloidal silica into the carrier (batch 9) or the use of a smaller grade of milled lactose (Lac_{200}, batch 10) led to a decreased nanoparticle recovery or very loose granules. Hence, a medium size milled lactose monohydrate quality (Lac) was finally chosen as carrier for further trials.

The batch size was kept at a small amount of around 0.17 kg for each granulation trial. Parameters for the spraying rate and the atomization air pressure were set based on preliminary nanoparticle free experiments (granulation with PVA solution). A product temperature of 35 °C was chosen for the first experiments. Later measurements showed that the T_g of the nanoparticles in aqueous suspension was only around 30 °C (data not shown). The T_g values therefore were in accordance with already published data [42]. Granulation trials with the same formulations and parameters led to granules with an equal nanoparticle release when performed slightly below (25 °C) or above (35 °C) this value (Table 2, batch 1 vs. 3 and batch 2 vs. 4). The product temperature was kept at 25 °C for the following experiments as a precaution to avoid a temperature related coalescence of the particles.

3.1.3. Tableting and encapsulation of nanoparticle containing granules

The aim was to produce tablets with a release of nanoparticles as high as possible, an average mass of 500 mg, with a fast disintegration, and with a breaking strength and friability values allowing an optional coating step. The first tablets were prepared from 95% nanoparticle-containing granules produced of different carriers and 5% extra-granular excipients. They showed distinct differences already in the disintegration test: lactose tablets and DCPA tablets quickly disintegrated to non-dissolving microparticles. In contrast, lactose/poloxamer tablets swelled and formed insoluble matrices that were stable for more than 4 h testing and showed dry masses of about the amount of PLGA per tablet. This phenomenon was attributed to a pressure dependent coagulation of the PLGA-coated particle surfaces as reported for the compression of formulations containing high loads of polymer-coated pellets [43]. There was no measurable recovery of nanoparticles from the lactose/poloxamer and DCPA tablets. That was in accordance with the SEM images of those samples (Fig. 3E, F) and their disintegration results. However, even lactose tablets containing well releasing granules showed a bad nanoparticle recovery of only around 10% compared to the unprocessed granules in dissolution test. The

Table 3
Settings and results of DoE granulation experiments.

Batch [no]	Carrier	PVA type	Factors PVA content of granules [%]	Product temperature [°C]	PLGA content of granules [%]	Spraying rate [g/min]	Atomization air pressure [bar]	Results Yield [%]	Mean particle size [µm]	Bulk density [g/ml]	Flowability [cot°]	NP release [%]
DoE 1	Lac	4-88	2.5	25	5.8	2.5	1.4	91	304	0.38	1.39	78 ± 11
DoE 2					8.2	3.7	0.8	99	610	0.22	1.19	69 ± 6
DoE 3					5.8	3.7	0.8	98	580	0.21	1.06	93 ± 1
DoE 4					7.0	3.1	1.1	96	353	0.32	1.16	74 ± 3
DoE 5					8.2	2.5	0.8	95	458	0.25	1.04	64 ± 2
DoE 6					8.2	2.5	1.4	73	274	0.43	1.28	46 ± 12
DoE 7					7.0	3.1	1.1	94	354	0.31	1.19	82 ± 7
DoE 8					7.0	3.1	1.1	96	380	0.29	1.22	75 ± 3
DoE 9					5.8	2.5	0.8	96	478	0.24	1.14	94 ± 2
DoE 10					5.8	3.7	1.4	97	386	0.26	1.19	91 ± 1
DoE 11					8.2	3.7	1.4	94	296	0.38	1.22	59 ± 9

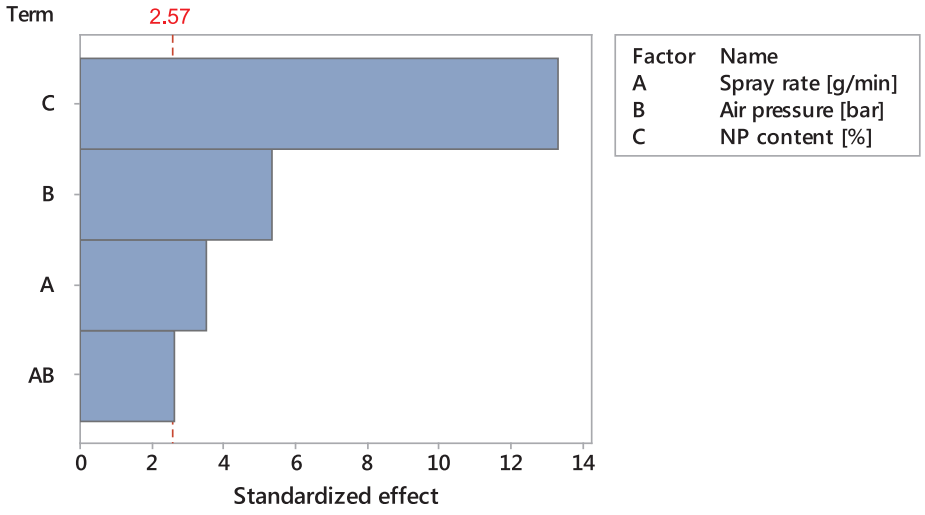

Fig. 5. Pareto diagram of standardized effect regarding the release of nanoparticles from the DoE granules. Answer is NP released from granules [%]; α = 0.05.

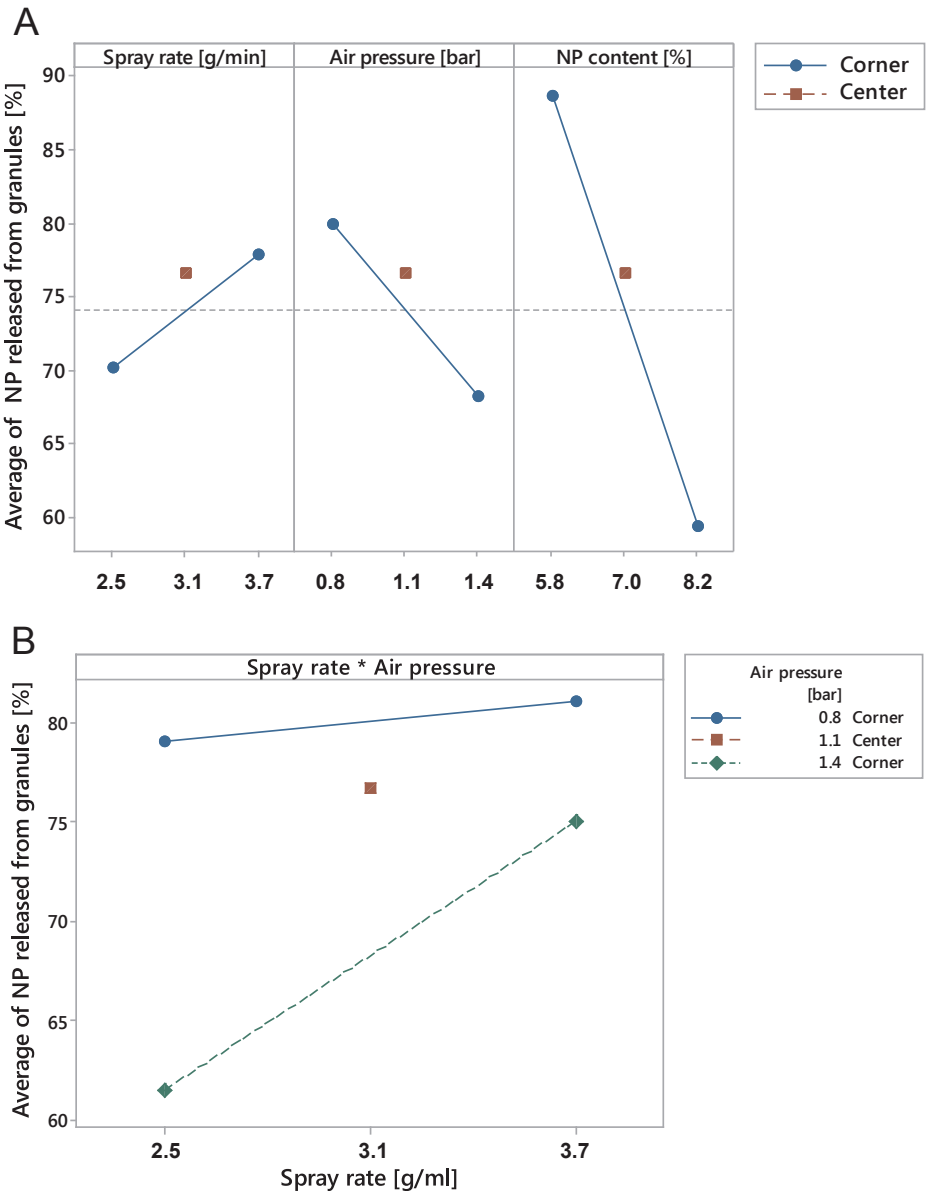

Fig. 6. Main effects diagram (A) and interaction diagram of the factors spray rate and atomization air pressure (B) for NP released from granules [%].

Table 4
Settings and results of granulation experiments extending prior design space.

Batch [no]	Carrier	PVA type	PVA content of granules [%]	Product temperature [°C]	PLGA content of granules [%]	Spraying rate [g/min]	Atomization air pressure [bar]	Yield [%]	Mean particle size [µm]	Bulk density [g/ml]	Flowability [cot°]	NP release [%]
11	Lac	4–88	2.5	25	5.8	4.4	0.8	98	612	0.23	1.09	94 ± 1
12			2.5		5.8	5.1	0.8	98	671	0.22	1.04	92 ± 2
13			2.5		5.8	5.2	1.4	96	496	0.26	1.09	97 ± 2
14			3.5		8.2	5.1	1.4	96	587	0.24	1.09	92 ± 1

following three alternatives on the former tablet formulation and tableting process were tested to determine whether a pressure dependent film formation was responsible for that strongly declined recovery: (1) the plastic filler and cushioning agent MCC was incorporated into the formulation to separate the granule particles and thus to avoid a film formation at their contact points, also to absorb some tableting energy and to reduce the forces required to obtain robust tablets, (2) tablets were produced with a wider range of target breaking strength to evaluate the influence of the compression force on the dissolution behavior, and (3) either the granules or the final blend containing MCC were filled into HPMC capsules and tested for dissolution as alternative oral dosage form prepared with very low tamping forces of maximum 60 N. Tablets prepared from the granules of batch 6 with 86 ± 1% nanoparticle recovery that contained only 60% granules but 35% plastic filler showed a nanoparticle recovery quite near to that of the original granules: 63–75% mean recovery. Furthermore, a lower breaking strength (correlating with lower compression forces) seemed to improve the release from the tablets: 63 ± 5% recovery at 107 N mean breaking strength, 68 ± 2% at 80 N and 75 ± 9% at 59 N.

Unexpectedly, the encapsulation approach led to a low nanoparticle recovery. That was ascribed to the observed incomplete disintegration of the plugs. The capsules with the final blend containing some disintegrant showed slightly higher release (41 ± 8%) than the capsules filled with the pure granules (28 ± 1%). Still, both formulations showed only little release when compared with the tablets though the tablets were prepared using much higher compression forces. This finding was attributed to the swelling behavior of PLGA nanoparticles reported by other authors [44]. It was assumed that water diffusion through the dissolving HPMC capsule's shell already led to a gelling polymeric network. The resulting capsule-shaped matrices therefore showed an incomplete particle release whereas the tablets containing MCC were disrupted shortly after the contact with water. Henceforth, only tableting was further investigated for converting the nanoparticle containing granules into solid dosage forms. The addition of a plastic filler at different levels and different target breaking strengths were selected as factors for a tableting DoE to be performed after further evaluation of the granulation step.

3.2. Optimization of drying and further downstreaming process

A general requirement for the use of AF4 and especially PCS in this study was the reproducible size and narrow range of diameter values (estimated by PDI) of the PLGA nanoparticle suspensions as well as of the particles released from the solid dosage forms. As shown in Fig. 3D and Fig. 4, the nanoparticles released during dissolution testing showed very similar diameter values compared to those of the original suspension. The PDI values increased over downstreaming but were below values of 0.2 and therefore acceptable even for tablets compressed with high compression force. This allowed further experiments to be analyzed by PCS/AF4 with the formulation from the preliminary trials.

3.2.1. Fluid bed granulation

All DoE experiments regarding the fluid bed granulation were performed according to the test plan. Though, one effect of changing the process parameters that was not numerically assessed but proved to be critical was the appearance of adhering fines on the product container. Such fine and sticky adhering occurred in the 'dry' experiments with low spray rate and high atomization air pressure. It seemed to be aggravated in combination with a higher nanoparticle concentration of the used granulation suspension. Still, the yield was reduced only in two of the 11 experiments (batch 1 and 6) as can be seen from the results of the experiments given in Table 3. Only the DoE 6 (a low spray rate combined with a high air pressure and nanoparticle concentration) led to a final yield below 90% of the theoretical weigh-out quantity. The DoE therefore was evaluated as previously planned focusing on the main criteria and granules properties which were first of all the

Table 5
Settings and results of tableting.

Batch [no]	NP release granules [%]	Target breaking strength [N]	MCC [%]	Height [mm]	Mass [mg]	Friability 4 min [%]	Friability 20 min [%]	Disintegration [min]	NP release [%]
DoE 1	78 ± 11	60	0	5.6	509 ± 14	0.2	1.7	3.5	62 ± 5
		110		5.1–5.2	509 ± 11	0.0	0.3	14.0	30 ± 3
		85	23	5.5–5.6	511 ± 10	0.0	0.3	0.5	61 ± 1
		60	45	6.2–6.3	508 ± 9	0.1	0.8	0.2	76 ± 7
		110		5.7–5.8	499 ± 13	0.0	0.3	0.4	73 ± 4
DoE 2	69 ± 6	60	0	5.5–5.6	507 ± 7	0.1	1.0	2.0	40 ± 4
		110		5.2–5.3	500 ± 8	0.1	0.3	36.0	20 ± 2
		85	23	5.6–5.7	505 ± 13	0.1	0.7	0.8	46 ± 5
		60	45	6.3–6.4	503 ± 11	0.3	3.1	0.3	67 ± 6
		110		5.7–5.8	502 ± 10	0.0	0.2	0.2	54 ± 5
DoE 3	93 ± 1	60	0	5.6	505 ± 9	0.2	1.6	2.5	60 ± 6
		110		5.3	508 ± 8	0.1	0.4	100.0	44 ± 5
		85	23	5.6–5.8	509 ± 8	0.1	0.6	0.4	79 ± 7
		60	45	6.3–6.5	504 ± 10	0.2	2.1	0.2	79 ± 8
		110		5.8	509 ± 12	0.1	0.4	0.5	70 ± 7
DoE 4	74 ± 3	60	0	5.6	499 ± 5	0.3	1.8	4.0	45 ± 3
		110		5.2–5.3	502 ± 6	0.0	0.3	85.0	26 ± 2
		85	23	5.8	499 ± 7	0.1	1.1	0.9	64 ± 5
		60	45	6.3–6.4	502 ± 4	0.2	1.8	0.3	71 ± 5
		110		5.8–5.9	502 ± 7	0.1	0.4	0.3	62 ± 9
DoE 5	64 ± 2	60	0	5.5–5.6	509 ± 9	0.3	1.9	10.0	29 ± 1
		110		5.2–5.3	507 ± 11	0.1	0.6	43.0	14 ± 3
		85	23	5.6–5.7	504 ± 14	0.1	0.6	1.0	38 ± 4
		60	45	6.2–6.3	503 ± 7	0.1	0.9	0.3	49 ± 8
		110		5.7–5.8	508 ± 13	0.0	0.5	0.4	40 ± 2
DoE 6	46 ± 12	60	0	5.4–5.5	509 ± 9	0.2	1.1	30.0	16 ± 1
		110		5.1–5.2	507 ± 11	0.0	0.4	80.0	6 ± 1
		85	23	5.6	504 ± 14	0.0	0.4	0.7	28 ± 3
		60	45	6.1–6.2	503 ± 7	0.0	0.5	0.2	41 ± 1
		110		5.7–5.8	508 ± 13	0.0	0.1	0.3	29 ± 2
DoE 7	82 ± 7	60	0	5.5–5.6	497 ± 9	0.2	1.3	3.0	46 ± 2
		110		5.1–5.2	503 ± 9	0.0	0.3	50.0	19 ± 2
		85	23	5.6	501 ± 8	0.1	0.6	1.0	54 ± 5
		60	45	6.3	501 ± 4	0.1	1.1	0.2	79 ± 10
		110		5.8	499 ± 6	0.0	0.1	0.3	57 ± 5
DoE 8	75 ± 3	60	0	5.5–5.6	503 ± 6	0.2	1.2	2.0	47 ± 3
		110		5.2	503 ± 7	0.1	0.3	8.0	23 ± 1
		85	23	5.6	498 ± 9	0.1	0.5	0.5	56 ± 6
		60	45	6.3–6.4	502 ± 9	0.2	1.7	0.3	72 ± 7
		110		5.7–5.8	499 ± 6	0.0	0.1	0.4	61 ± 6
DoE 9	94 ± 2	60	0	5.5–5.6	508 ± 9	0.2	1.2	1.5	57 ± 5
		110		5.1–5.2	505 ± 10	0.0	0.3	15.0	29 ± 4
		85	23	5.6	506 ± 9	0.1	0.6	0.5	68 ± 4
		60	45	6.2–6.3	501 ± 8	0.1	1.1	0.3	88 ± 4
		110		5.7–5.8	506 ± 9	0.0	0.1	0.4	81 ± 10
DoE 10	91 ± 1	60	0	5.5–5.6	504 ± 7	0.1	1.2	1.3	54 ± 2
		110		5.1–5.2	506 ± 9	0.1	0.3	24.0	27 ± 3
		85	23	5.6–5.7	505 ± 12	0.1	0.6	0.6	68 ± 3
		60	45	6.2–6.3	505 ± 8	0.2	1.6	0.3	84 ± 5
		110		5.8	506 ± 11	0.0	0.2	0.6	72 ± 4
DoE 11	59 ± 9	60	0	5.6	505 ± 10	0.3	1.8	7.0	33 ± 2
		110		5.2–5.3	505 ± 10	0.1	0.5	60.0	14 ± 2
		85	23	5.6–5.7	505 ± 7	0.1	0.7	1.0	39 ± 3
		60	45	6.2–6.3	512 ± 14	0.0	0.7	0.3	56 ± 4
		110		5.7–5.8	513 ± 22	0.1	0.4	0.8	45 ± 3

recovery of the nanoparticles, the mean granules size and the density.

The DoE granules showed a wide range of mean particle sizes (274–610 µm) and bulk densities (0.21–0.41 g/ml) due to the relatively broad ranges of the design space. The mean particle size was significantly influenced by the synergistic factor spray rate and the antagonistic factor atomization air pressure. The bulk density of the DoE granules was in inverse proportion to the mean size and was significantly influenced by the synergistic factor atomization air pressure. Independent of the granulation parameters the loss on drying (LoD) of the studied granules was only 0.53 ± 0.06% and therefore no impact on the nanoparticle recovery or the subsequent compaction process was expected.

The recovery of nanoparticles during dissolution as the most important quality attribute was primarily influenced by the nanoparticle concentration of the granulation suspension while the spray rate, the atomization air pressure and their interaction had significant but lesser influence (Fig. 5).

As shown in the main effects diagram in Fig. 6A, a higher nanoparticle concentration in the granulation suspension and thus in the granules led to a drastically declined recovery within the design space. A higher spray rate rather increased the nanoparticle recovery whereas a higher atomization air pressure decreased the recovery. All those relations between the factors and the response recovery were found to be quite linear.

Higher spray rates might have fostered the recovery due to higher process humidity and larger droplets leading to faster nucleation, less spray drying and abrasion. It perhaps also facilitated the wettability and the adhesion of nanoparticles on the wetted carrier surface. The

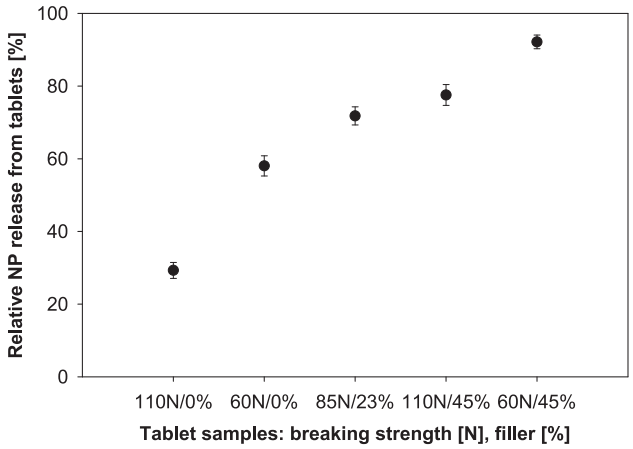

Fig. 7. Relative recovery of nanoparticles from DoE tablets (mean ± 95% CI).

negative effect of a higher atomization air pressure was attributed to the opposite effects plus the risk of above mentioned adhering fines and higher shear forces. Still, higher levels of atomization air pressure were generally seen as necessary for processing this formulation to achieve granules with mean sizes and densities adequate for further use. The interaction diagram in Fig. 6B indicated that the negative impact of the higher level of atomization air pressure compared to the lower level was distinctly diminished when combined with the higher level of spray rate. That implied rather a dependence of the process on a good or reasonable ratio of air pressure and spray rate than a *per se* bad influence of higher air pressure.

The higher level of nanoparticles in the granulation suspensions might have decreased the nanoparticle recovery by promoting agglomeration. This could have occurred due to increased closeness in the granulation suspension and on the carrier surface. Furthermore, the stabilizer to polymer ratio was slightly decreased. A different behavior of adhesion due to the changed surface hydrophobicity once the carrier particle was coated with PLGA was also assumed to be a possible factor for an increased cohesion and agglomeration on the particle surface. The importance of the surface hydrophobicity for coating processes has been widely investigated, e.g. when using higher drug loads in drying SMEDDS or nanocrystals [24,26].

As shown for the central point experiments in Table 3, the use of the same factor levels led to granules very much alike each other throughout the DoE: 77 ± 4% nanoparticle recovery, 362 ± 15 µm mean particle size and 0.30 ± 0.02 g/ml bulk density. All granules from the DoE could be compressed according to the plan, despite the wide range of granule size distributions and densities achieved. Before focusing on the compression step, some trials outside the DoE and its design space shall be mentioned. Those were performed to firstly test whether an increase in the spray rate enabled a higher level of atomization air pressure without impairing the nanoparticle recovery. Secondly, it was evaluated whether the higher nanoparticle loading of the final granules or the higher nanoparticle concentration of the used granulation suspension had induced the bad nanoparticle recovery found for the respective granules in the DoE.

As shown in Table 4, two granules were produced using spray rates exceeding the higher DoE level while maintaining the lower level of the atomization air pressure and the lower concentration of nanoparticles (batch 11 and 12). The resulting granules showed a high nanoparticle recovery and could be processed without any process issues but however showed comprehensibly low bulk densities and high mean particle sizes. A subsequent granulation, batch 13, was produced using the high spray rate from batch 12 combined with the higher level of atomization air pressure used in the DoE. The resulting granules had more advantageous particle properties while keeping a high nanoparticle recovery. A ratio of the atomization air volume and the spray rate was determined that was reasonable in means of the processability (avoiding fine adhering) and the particle data based on this test and the previous ones. The factor of the fluid flow divided by the air flow (both in g/min) multiplied with ten was set at ≥2.5.

The following test, batch 14, was conducted using the spraying parameters from batch 13 and a larger volume of low concentrated granulation suspension. This led to final granules with the same higher level of nanoparticles as the poor releasing granules from the DoE (DoE 2, 5, 6 and 11). In contrast to the latter, the granules of batch 14 showed a good nanoparticle recovery of more than 90% of the theoretically expected value. This finding supported the assumption that the concentration of the granulation suspension was the main factor affecting the extent of the later release of originally sized nanoparticles. The loading of the final granules itself may be important too, but was not the release limiting factor inside the evaluated design space.

3.2.2. Tableting

The tableting of the DoE granules should be performed using two factors with the experience from the preliminary trials: Firstly, the target breaking strength with 60, 85 and 110 N mean values for the lower, central point and higher level. Secondly, the incorporation of MCC into the final blends at a level of 0, 23 and 45% should be evaluated for each lot of the DoE granules. The most interesting quality attributes were the relative nanoparticle recovery after compression (relating to the nanoparticle release from the used granules) and the properties of the suspension formed after resuspending, namely the nanoparticle diameter and the PDI. The latter values were comparable to the original nanoparticle suspensions, as already shown in Fig. 4:

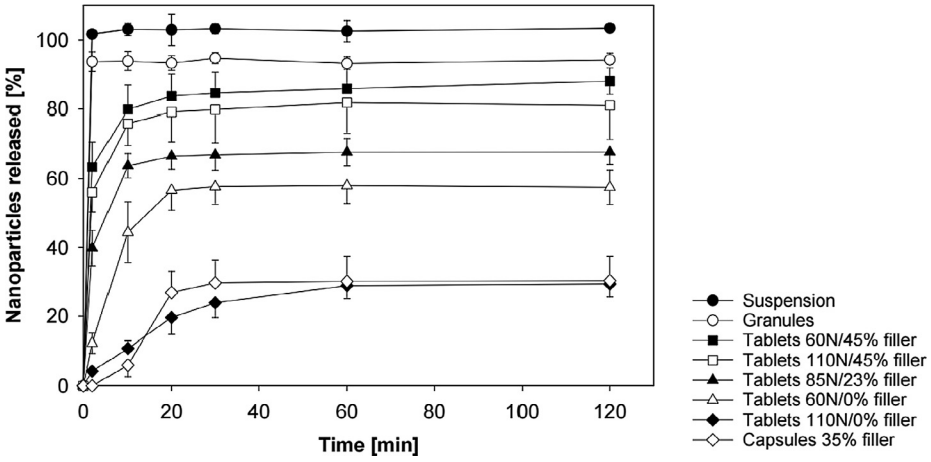

Fig. 8. Nanoparticle recovery after dissolution of different dosage forms of the same batch (DoE 9) (mean ± SD).

203 ± 2 nm/0.59 ± 0.019 for the suspensions, 199 ± 1 nm/0.078 ± 0.011 for the granules and 208 ± 3 nm/0.110 ± 0.019 for the tablets. The PDI values increased during downstreaming indicating some particle agglomeration during the drying and the compression process. However, those values will not be discussed here further because the different tablet samples did not show significant differences of mean PDI among each other depending on the level of MCC and breaking strength. Other quality attributes determined were the uniformity of mass, the disintegration time, the dimensions of the tablets and the friability after 4 min and, more predicative in terms of suitability of the cores for coating, after 20 min. The LoD of the different tablet samples depended alone on the amount of added MCC: 0.79 ± 0.16%, (0% MCC), 1.63 ± 0.17% (23% MCC) and 2.45 ± 0.28% (45% MCC). These moisture levels are considered uncritical taking into account usual LoD levels of commercial tablets from similar composition and, therefore, no impact on the physical properties of the tablets had to be expected.

Varying compression forces were expected to be required to form tablets of the same breaking strength due to the different amount of MCC. That would be observable by a different tablet height and calculated tablet density. Still, the same breaking strength for tablets consisting of different formulations should ideally lead to a comparable robustness and friability. The quality attributes for the tablets prepared from the DoE granules are given in Table 5. An analysis revealed that the nanoparticle release from the DoE tablets was depending on the granuleś quality (release from the respective DoE granules compressed), the level of plastic filler in the formulation and the breaking strength. A low breaking strength and an addition of MCC improved the nanoparticle release. The relative nanoparticle release from the tablets (absolute percentage recovery from the tablet sample divided by the absolute percentage recovery from the respective granules multiplied by 100) was depicted in Fig. 7. The relative release was shown to highlight the influence of the tableting parameters and to grade the important factor granuleś quality. As shown exemplary in Fig. 8, the tablet's dissolution rate curves showed distinct differences for the formulations. The trend of the dissolution rate curves was quite the same for all tablets with the same tableting factor levels though the extent of release strongly depended on the compressed granules: formulations including MCC showed a fast disintegration and reached the final dissolution plateau in 10–20 min. Samples without MCC often reached that plateau only after 30–60 min. Additionally, the different required compression forces for the two levels of the breaking strength were more obvious in case of the formulation without MCC: the 110 N samples often formed matrices with slow or incomplete disintegration. The eleven tablet samples with low breaking strength and high MCC content showed 92 ± 7% mean nanoparticle recovery relative to that of their original granules (data not shown). Thus, the 'tableting damage' observed in the preliminary tableting tests was very low with around mean 8% loss during that process step.

In a preliminary study the poorly soluble porphyrin derivative 5,10,15,20-tetrakis(m-hydroxyphenyl) porphyrin (*m*THPC), approved for photodynamic therapy, was incorporated into the nanoparticle system at an drug-to-PLGA ratio of 0.3 to 1 [37]. Although the incorporation of the drug led to a slight increase in nanoparticle diameter (225 ± 6 nm, PDI 0.099 ± 0.007), the use of drug-loaded instead of blank nanoparticle suspension did not alter the properties. In particular the release profile of the resulting granules was similiar to drug-free trials when using the same spraying parameters. However, tablets compressed with 5% outer phase and 45% MCC at a breaking strength of 60 N showed a somewhat reduced recovery of the nanoparticles when compared to similar drug-free trials (data not shown). Therefore, the transferability of our results with blank nanoparticles to drug-loaded ones may depend on the properties of a drug compound to be processed.

In the case of tablets based on granules with blank nanoparticles the factor breaking strength was used as a marker for the required compression force as that force was not reasonably adjustable for the very small amounts of the final blend. The other two markers, the tablet height and the calculated tablet density correlated with the nanoparticle release from the tablets too, the first directly and the latter inversely.

Based on the DoE data, a multiple regression was performed with the x variables x_1 nanoparticle release from the granules used for the final blend in percent, x_2 breaking strength in Newton and x_3 level of MCC in percent. The nanoparticle release from the tablets Y [%] could be described by the following equation:

$$Y = -13.6 + 1.566\,x_1 - 0.4159\,x_2 + 0.393\,x_3 - 0.00575\,x_1^2 - 0.00970\,x_3^2 + 0.00457\,x_1x_3 + 0.00391\,x_2x_3.$$

The calculated nanoparticle release for tableting trials prior and after the DoE were in good agreement with the empirical values, even when the factor settings were outside the design space of the DoE.

4. Conclusion

In summary, it can be stated that aqueous PLGA nanoparticle suspensions were successfully converted into dried form using fluid bed granulation. Formulation and process parameters were optimized to achieve a high nanoparticle release from its dosage form using statistical design of experiments. Soluble carriers for the granulation such as lactose were found to benefit a relevant recovery of nanoparticles from the granules. The factors most pronounced regarding the nanoparticle release from the granules or the processability and the powder data were determined. The same was done for the compression step.

The finally selected process parameters led to high yields of granules and a high release of original-sized nanoparticles from the granules. The most critical factor regarding the nanoparticle release during the granulation step was the nanoparticle content in the granulation suspension. Higher levels of nanoparticles in the suspension led to a reduced nanoparticle recovery. The negative impact of a higher level of atomization air pressure could be compensated when combined with a higher level of spray rate.

The granules were compressed to tablets and the nanoparticle release from the tablets was investigated. The highest nanoparticle release from the tablets was achieved in the presence of comparable high amounts of the filler MCC in combination with a low tablet breaking strength.

Additional experiments in future studies should be performed in order to prove the suitability of the described downstreaming process for other nanoparticle formulations for the oral route of application.

Acknowledgements

The authors acknowledge the German Bundesministerium für Bildung und Forschung (BMBF) for funding (FKZ 13N11385 and 13N11390). Furthermore, the authors like to thank Karin Possemeyer from the University of Muenster (Germany) for support with scanning electron microscopy.

References

[1] A.C. Fonseca, A.C. Serra, J.F. Coelho, Bioabsorbable polymers in cancer therapy: latest developments, EPMA J. 6 (2015) 22.
[2] H. Maeda, K. Tsukigawa, J. Fang, A retrospective 30 years after discovery of the enhanced permeability and retention effect of solid tumors: next-generation chemotherapeutics and photodynamic therapy—problems, solutions, and prospects, Microcirculation 23 (2016) 173–182.
[3] F. Masood, Polymeric nanoparticles for targeted drug delivery system for cancer therapy, Mater. Sci. Eng. C Mater. Biol. Appl. 60 (2016) 569–578.
[4] R.C. Mundargi, V.R. Babu, V. Rangaswamy, P. Patel, T.M. Aminabhavi, Nano/micro technologies for delivering macromolecular therapeutics using poly(D, L-lactide-co-glycolide) and its derivatives, J. Control. Release 125 (2008) 193–209.
[5] F. Danhier, E. Ansorena, J.M. Silva, R. Coco, A. Le Breton, V. Preat, PLGA-based nanoparticles: an overview of biomedical applications, J. Control. Release 161

(2012) 505–522.
[6] N.M. Khalil, T.C. do Nascimento, D.M. Casa, L.F. Dalmolin, A.C. de Mattos, I. Hoss, M.A. Romano, R.M. Mainardes, Pharmacokinetics of curcumin-loaded PLGA and PLGA-PEG blend nanoparticles after oral administration in rats, Colloids Surf. B Biointerfaces 101 (2013) 353–360.
[7] N. Ubrich, C. Schmidt, R. Bodmeier, M. Hoffman, P. Maincent, Oral evaluation in rabbits of cyclosporin-loaded Eudragit RS or RL nanoparticles, Int. J. Pharm. 288 (2005) 169–175.
[8] M. Wang, Y. Zhang, J. Feng, T. Gu, Q. Dong, X. Yang, Y. Sun, Y. Wu, Y. Chen, W. Kong, Preparation, characterization, and in vitro and in vivo investigation of chitosan-coated poly (d, l-lactide-co-glycolide) nanoparticles for intestinal delivery of exendin-4, Int. J. Nanomedicine 8 (2013) 1141–1154.
[9] N. Reix, A. Parat, E. Seyfritz, R. Van der Werf, V. Epure, N. Ebel, L. Danicher, E. Marchioni, N. Jeandidier, M. Pinget, Y. Frere, S. Sigrist, In vitro uptake evaluation in Caco-2 cells and in vivo results in diabetic rats of insulin-loaded PLGA nanoparticles, Int. J. Pharm. 437 (2012) 213–220.
[10] E.M. Pridgen, F. Alexis, T.T. Kuo, E. Levy-Nissenbaum, R. Karnik, R.S. Blumberg, R. Langer, O.C. Farokhzad, Transepithelial transport of Fc-targeted nanoparticles by the neonatal fc receptor for oral delivery, Sci. Transl. Med. 5 (2013) 213ra167.
[11] S. Sun, N. Liang, H. Yamamoto, Y. Kawashima, F. Cui, P. Yan, pH-sensitive poly (lactide-co-glycolide) nanoparticle composite microcapsules for oral delivery of insulin, Int. J. Nanomedicine 10 (2015) 3489–3498.
[12] Y.I. Kim, L. Fluckiger, M. Hoffman, I. Lartaud-Idjouadiene, J. Atkinson, P. Maincent, The antihypertensive effect of orally administered nifedipine-loaded nanoparticles in spontaneously hypertensive rats, Br. J. Pharmacol. 120 (1997) 399–404.
[13] V. Zabaleta, G. Ponchel, H. Salman, M. Agueros, C. Vauthier, J.M. Irache, Oral administration of paclitaxel with pegylated poly(anhydride) nanoparticles: permeability and pharmacokinetic study, Eur. J. Pharm. Biopharm. 81 (2012) 514–523.
[14] V. Bourganis, T. Karamanidou, E. Samaridou, K. Karidi, O. Kammona, C. Kiparissides, On the synthesis of mucus permeating nanocarriers, Eur. J. Pharm. Biopharm. 97 (2015) 239–249.
[15] I. Pereira de Sousa, C. Steiner, M. Schmutzler, M.D. Wilcox, G.J. Veldhuis, J.P. Pearson, C.W. Huck, W. Salvenmoser, A. Bernkop-Schnürch, Mucus permeating carriers: formulation and characterization of highly densely charged nanoparticles, Eur. J. Pharm. Biopharm. 97 (2015) 273–279.
[16] L. Inchaurraga, N. Martin-Arbella, V. Zabaleta, G. Quincoces, I. Penuelas, J.M. Irache, In vivo study of the mucus-permeating properties of PEG-coated nanoparticles following oral administration, Eur. J. Pharm. Biopharm. 97 (2015) 280–289.
[17] C. Damge, C. Michel, M. Aprahamian, P. Couvreur, J.P. Devissaguet, Nanocapsules as carriers for oral peptide delivery, J. Control. Release 13 (1990) 233–239.
[18] M.S. Cartiera, K.M. Johnson, V. Rajendran, M.J. Caplan, W.M. Saltzman, The uptake and intracellular fate of PLGA nanoparticles in epithelial cells, Biomaterials 30 (2009) 2790–2798.
[19] G. Ponchel, M. Montisci, A. Dembri, C. Durrer, D. Duchene, Mucoadhesion of colloidal particulate systems in the gastro-intestinal tract, Eur. J. Pharm. Biopharm. 44 (1997) 25–31.
[20] W. Abdelwahed, G. Degobert, S. Stainmesse, H. Fessi, Freeze-drying of nanoparticles: formulation, process and storage considerations, Adv. Drug Deliv. Rev. 58 (2006) 1688–1713.
[21] S. Wanning, R. Süverkrüp, A. Lamprecht, Pharmaceutical spray freeze drying, Int. J. Pharm. 488 (2015) 136–153.
[22] S. Basa, T. Muniyappan, P. Karatgi, R. Prabhu, R. Pillai, Production and in vitro characterization of solid dosage form incorporating drug nanoparticles, Drug Dev. Ind. Pharm. 34 (2008) 1209–1218.
[23] P. Kayaert, M. Anne, G. Van den Mooter, Bead layering as a process to stabilize nanosuspensions: influence of drug hydrophobicity on nanocrystal reagglomeration following in-vitro release from sugar beads, J. Pharm. Pharmacol. 63 (2011) 1446–1453.
[24] S. Bose, D. Schenck, I. Ghosh, A. Hollywood, E. Maulit, C. Ruegger, Application of spray granulation for conversion of a nanosuspension into a dry powder form, Eur. J. Pharm. Sci. 47 (2012) 35–43.
[25] C.E. Figueroa, S. Bose, Spray granulation: importance of process parameters on in vitro and in vivo behavior of dried nanosuspensions, Eur. J. Pharm. Biopharm. 85 (2013) 1046–1055.
[26] K. Cerpnjak, A. Zvonar Pobirk, F. Vrecer, M. Gasperlin, Tablets and minitablets prepared from spray-dried SMEDDS containing naproxen, Int. J. Pharm. 495 (2015) 336–346.
[27] R. Bodmeier, H.G. Chen, O. Paeratakul, A novel approach to the oral delivery of micro- or nanoparticles, Pharm. Res. 6 (1989) 413–417.
[28] C. Schmidt, R. Bodmeier, Incorporation of polymeric nanoparticles into solid dosage forms, J. Control. Release 57 (1999) 115–125.
[29] A. Engel, M. Plöger, D. Mulac, K. Langer, Asymmetric flow field-flow fractionation (AF4) for the quantification of nanoparticle release from tablets during dissolution testing, Int. J. Pharm. 461 (2014) 137–144.
[30] P. Merkku, A. Lindqvist, K. Leiviska, J. Yliruusi, Influence of granulation and compression process variables on flow rate of granules and on tablet properties, with special reference to weight variation, Int. J. Pharm. 102 (1994) 117–125.
[31] L. Suhrenbrock, G. Radtke, K. Knop, P. Kleinebudde, Suspension pellet layering using PVA-PEG graft copolymer as a new binder, Int. J. Pharm. 412 (2011) 28–36.
[32] V. Lourenco, D. Lochmann, G. Reich, J.C. Menezes, T. Herdling, J. Schewitz, A quality by design study applied to an industrial pharmaceutical fluid bed granulation, Eur. J. Pharm. Biopharm. 81 (2012) 438–447.
[33] I. Aleksic, J. Duris, S. Ibric, J. Parojcic, An investigation into the usefulness of different empirical modeling techniques for better control of spray-on fluidized bed melt granulation, Int. J. Pharm. 496 (2015) 627–635.
[34] A. Curic, B.L. Keller, R. Reul, J. Moschwitzer, G. Fricker, Development and lyophilization of itraconazole loaded poly(butylcyanoacrylate) nanospheres as a drug delivery system, Eur. J. Pharm. Sci. 78 (2015) 121–131.
[35] C. Draheim, F. de Crecy, S. Hansen, E.M. Collnot, C.M. Lehr, A design of experiment study of nanoprecipitation and nano spray drying as processes to prepare PLGA nano- and microparticles with defined sizes and size distributions, Pharm. Res. 32 (2015) 2609–2624.
[36] E.O. Akala, S. Adesina, O. Ogunwuyi, Computer optimization of biodegradable nanoparticles fabricated by dispersion polymerization, Int. J. Environ. Res. Public Health 13 (2015) ijerph13010047.
[37] J. Grünebaum, J. Söbbing, D. Mulac, K. Langer, Nanoparticulate carriers for photodynamic therapy of cholangiocarcinoma: in vitro comparison of various polymer-based nanoparticles, Int. J. Pharm. 496 (2015) 942–952.
[38] D. Jones, Process development, optimization and scale-up: Wurster coating, in: Y. Qiu, Y. Chen, G.G.Z. Zhang, L. Liu, W.R. Porter (Eds.), Developing solid oral dosage forms, Elsevier Inc., Amsterdam, Netherlands, 2009, pp. 807–825.
[39] M.I. Baker, S.P. Walsh, Z. Schwartz, B.D. Boyan, A review of polyvinyl alcohol and its uses in cartilage and orthopedic applications, J. Biomed. Mater. Res. B Appl. Biomater. 100 (2012) 1451–1457.
[40] J.S. LaFountaine, S.V. Jermain, L.K. Prasad, C. Brough, D.A. Miller, D. Lubda, J.W. McGinity, R.O. Williams 3rd, Enabling thermal processing of ritonavir-polyvinyl alcohol amorphous solid dispersions by KinetiSol(R) Dispersing, Eur. J. Pharm. Biopharm. 101 (2016) 72–81.
[41] G. Baki, J. Bajdik, D. Djuric, K. Knop, P. Kleinebudde, K. Pintye-Hodi, Role of surface free energy and spreading coefficient in the formulation of active agent-layered pellets, Eur. J. Pharm. Biopharm. 74 (2010) 324–331.
[42] S. Lappe, D. Mulac, K. Langer, Polymeric nanoparticles – influence of the glass transition temperature on drug release, Int. J. Pharm. 517 (2017) 338–347.
[43] M. Braun, Einflussfaktoren bei der Tablettierung magensaftresistent überzogener Pellets auf Exzenter- und Rundlauftablettenpresse, Mathematisch-Naturwissenschaftliche Fakultät, RFWU Bonn, Bonn, 2003.
[44] H. Murakami, M. Kobayashi, H. Takeuchi, Y. Kawashima, Utilization of poly(DL-lactide-co-glycolide) nanoparticles for preparation of mini-depot tablets by direct compression, J. Control. Release 67 (2000) 29–36.